Flight Stability Study of Micro Air Vehicle with Elastic Aerodynamic Shape

Yanan Yu [a,b], Qingping Yang [a], and Xiangjun Wang [b]
[a] School of Engineering and Design, Brunel University, London, UK
[b] State Key Laboratory of Precision Measuring Technology and Instruments, Tianjin University, Tianjin, China

***Abstract*—Flight stability of air vehicles is often considered a significant research issue during aircraft structure design process. In the attempt to improve such properties, the investigation of the effects the design parameters may have on the flight stability or anti-disturbance property has become a constituent part in design and testing stage. Micro air vehicles (MAVs) are small size unmanned aircraft, in which flight attitude and stability are more sensitive to the environmental disturbance. A vertical ducted-fan hovering MAV with an elastic aerodynamic shape was presented and discussed in this paper. Based upon a three-dimensional measurement method, a stroboscopic imaging technique was proposed and the spatial information of aircraft aerodynamic shape deformation has been obtained and presented. Then the effects of structural design parameters on the flight stability was analyzed and calculated mathematically. It was found that aircrafts simultaneously having a large height and small external radius of the shell have a relatively large deformation component in the aerodynamic shape under a given disturbance force. It also means that the flight stability of an aircraft with this characteristic can be improved.**

Keywords-micro air vehicle (MAV); aerodynamic shape; stroboscopic imaging technique; flight stability; parametric surface

I. INTRODUCTION

The micro air vehicles (MAVs) usually refer to the small scale, automatic, unmanned air vehicles [1]. In recent years, MAVs have played a significant role in military surveillance, environment monitoring, scientific mapping and other fields of the modern world [2]. Due to their small size and light weight MAVs are more sensitive to atmosphere disturbances than other types of aircrafts. Therefore, improving and assuring flight stability and anti-disturbance properties should be considered during the design process [3]. For example, in [4] the stability characteristics and the control properties of hovering MAVs in wind gusts are described. Testing using a wind tunnel is one of the most effective ways to obtain flight performances and analyze stability characteristics. Current experimental approaches are divided into contact and non-contact measurement. The contact method usually uses various force sensors to measure deformation or acting forces on the experimental model [5]. Non-contact measurement is primarily based upon visual measurement principle to realize high precision and speed [6].

The prime aim of this study is to establish a wind tunnel testing environment to obtain three-dimensional information, represent the aerodynamic shape surface parametrically, and moreover, investigate the effects of selected design parameters on the flight stability of an aero-elastic ducted-fan hovering MAV. Vertical take-off, landing and hover capabilities are the main characteristics of hovering MAVs [7]. The structure parameters will have a constituent part in the flight characteristics, especially when the aerodynamic shape having elastic deformations. Usually some shape definition problems are solved based upon the experimental estimation or mathematical computation. In Section II, the geometrical parameters of the hovering MAV design considered in this study are discussed. Its parametric surface is defined mathematically by two different function forms. In Section III, three-dimensional measurement system based upon stroboscopic imaging technique is introduced. By using this method, scale invariant feature transform (SIFT) features are extracted from the aerodynamic shape of the model and used to reconstruct the shape as well as to define parametric function. In Section IV, the relationship between geometrical design parameters and the deformation variable or flight stability is analyzed. The conclusions are then drawn in Section V.

II. GEOMETRY OF THE CONSIDERED HOVERING MAV

A. Geometrical Design parameters

The aircraft designed in this study is a vertical ducted-fan hovering MAV surrounded with elastic aerodynamic shape, which is shown in Fig.1. Under a disturbance force, the aerodynamic shape will have a deformation on its surface and the amount of deformation is relative with the pressure force. Due to the fluid-structure interaction existing between airflow and structure, the aerodynamic shape of the aircraft partly determines aircraft's fight stability, attitude and speed. So four dimensional parameters have been selected to investigate the effects they may have on the flight stability of the whole structure.

In Fig. 1, R is the external radius of the shell, r is the internal radius of the cylindrical vertical duct, H is the height of the aircraft and t is the thickness of the shell.

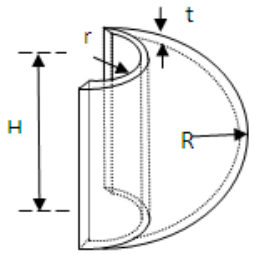

Figure 1. Designed parameters of the model

978-1-4577-1772-7/12/$26.00 ©2012 IEEE

B. Geometric form of definition

Ducted-fan hovering aircrafts look like a transformation of torus structure. Usually the equation of the torus structure is defined as (1),

$$\begin{cases} x(u,v) = (c + acosv)cosu \\ y(u,v) = (c + acosv)sinu \\ z(u,v) = asinv \end{cases} \quad (1)$$

where a is the radius of the tube and c is the distance from the centre of the tube to the centre of the torus, u and v are in the range of (0, 2π). Here u is the angle around the torus and v is the angle around the tube. Then the torus structure can be represented by (2):

$$P(u,v) = f\big(x(u,v), y(u,v), z(u,v)\big) \quad (2)$$
$$(0 < u < 2\pi, 0 < v < 2\pi)$$

During the design and manufacture process, various shapes and parameters should be considered due to their effects on the flight characteristics. Some design structures are presented in Table 1.

TABLE I. VARIOUS DESIGN STRUCTURES

The range of w	Structure model	Notes
$\frac{\pi}{2} < \|w\| < \pi$	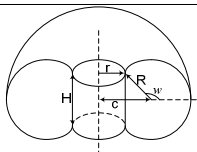	The centre of the shell is outside the vertical duct
$\|w\| = \frac{\pi}{2}$	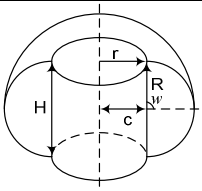	The centre of the shell is on the vertical duct
$\arccos(\frac{r}{a}) < \|w\| < \frac{\pi}{2}$	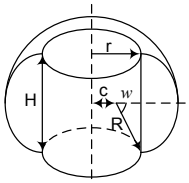	The centre of the shell is inside the vertical duct
$\|w\| = \arccos(\frac{r}{a})$	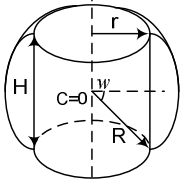	The centre of the shell is on the axis of the vertical duct
$0 < \|w\| < \arccos(\frac{r}{a})$	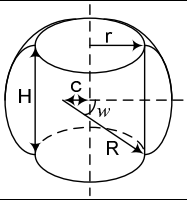	The centre of the shell is inside the vertical duct

The external radius R of the shell equals the radius of the tube, a, and the internal radius of the cylindrical vertical duct r is calculated by (3), where w is in the interval (-π, π). The height of the aircraft H is calculated by (4):

$$\begin{cases} r = c + acosw, \arccos\left(\frac{r}{a}\right) \le |w| < \pi \\ r = acosw - c, 0 < |w| < \arccos\left(\frac{r}{a}\right) \end{cases} \quad (3)$$

$$H = 2asinw \quad (4)$$

So the value c can be obtained easily from each structure. Substituting the values of a and c in (1) respectively, the parametric definition of the designed aircraft is given as:

$$\begin{cases} \begin{cases} x(u,v) = \left(r + \sqrt{R^2 - \frac{H^2}{4}} + Rcosv\right)cosu \\ y(u,v) = \left(r + \sqrt{R^2 - \frac{H^2}{4}} + Rcosv\right)sinu \\ z(u,v) = Rsinv \end{cases}, & \frac{\pi}{2} < |w| < \pi \\ \begin{cases} x(u,v) = \left(r - \sqrt{R^2 - \frac{H^2}{4}} + Rcosv\right)cosu \\ y(u,v) = \left(r - \sqrt{R^2 - \frac{H^2}{4}} + Rcosv\right)sinu \\ z(u,v) = Rsinv \end{cases}, & \arccos\left(\frac{r}{R}\right) \le |w| \le \frac{\pi}{2} \\ \begin{cases} x(u,v) = \left(\sqrt{R^2 - \frac{H^2}{4}} - r + Rcosv\right)cosu \\ y(u,v) = \left(\sqrt{R^2 - \frac{H^2}{4}} - r + Rcosv\right)sinu \\ z(u,v) = Rsinv \end{cases}, & 0 < |w| < \arccos\left(\frac{r}{R}\right) \end{cases} \quad (5)$$

where u is in the range (0, 2π) and v is in the range (-|w|, |w|).

C. Algebraic form of definition

A parametric surface is a space patch which is defined by a parametric equation with several parameters. Continuous parametric variable u and v are used as the coordinates of some part of a plane and x, y, z are used as the usual Cartesian coordinates. A parametric surface can be established by (6):

$$P(u,v) = f(x,y,z) \quad (6)$$

where $x = x(u,v)$, $y = y(u,v)$, $z = z(u,v)$, the parametric variables u and v are in the range of (0,1). The algebraic form of a bi-cubic patch is as:

$$\begin{cases} x(u,v) = a_{33x}u^3v^3 + a_{32x}u^3v^2 + \cdots + a_{00x} \\ y(u,v) = a_{33y}u^3v^3 + a_{32y}u^3v^2 + \cdots + a_{00y} \\ z(u,v) = a_{33z}u^3v^3 + a_{32z}u^3v^2 + \cdots + a_{00z} \end{cases} \quad (7)$$

$$u \in (0,1), v \in (0,1)$$

Let the points be (x_1 y_1 z_1), (x_2 y_2 z_2)…(x_{16} y_{16} z_{16}) and their respective parametric values are (u_1 v_1), (u_2 v_2)…(u_{16} v_{16}). So the x coordinate of the bi-cubic patch can be rewritten as (8):

$$\begin{bmatrix} u_1^3v_1^3 & u_1^3v_1^2 \cdots & v_1 & 1 \\ u_2^3v_2^3 & u_2^3v_2^2 & v_2 & 1 \\ \vdots & & \vdots & 1 \\ u_{16}^3v_{16}^3 & u_{16}^3v_{16}^2 \cdots & v_{16} & 1 \end{bmatrix} \begin{bmatrix} a_{33x} \\ a_{32x} \\ \vdots \\ a_{00x} \end{bmatrix} = \begin{bmatrix} x_1 \\ x_2 \\ \vdots \\ x_{16} \end{bmatrix} \quad (8)$$

$$\begin{bmatrix} a_{33x} \\ a_{32x} \\ \vdots \\ a_{00x} \end{bmatrix} = \begin{bmatrix} u_1^3v_1^3 & u_1^3v_1^2 \cdots & v_1 & 1 \\ u_2^3v_2^3 & u_2^3v_2^2 & v_2 & 1 \\ & \vdots & \vdots & 1 \\ u_{16}^3v_{16}^3 & u_{16}^3v_{16}^2 \cdots & v_{16} & 1 \end{bmatrix}^{-1} \begin{bmatrix} x_1 \\ x_2 \\ \vdots \\ x_{16} \end{bmatrix} \quad (9)$$

The coefficient matrix $A_x = \begin{bmatrix} a_{33x} & a_{32x} & a_{31x} & a_{30x} \\ a_{23x} & a_{22x} & a_{21x} & a_{20x} \\ a_{13x} & a_{12x} & a_{11x} & a_{10x} \\ a_{03x} & a_{02x} & a_{01x} & a_{00x} \end{bmatrix}$ can be calculated by (9). The treatment for A_y and A_z coefficient matrices are similar.

III. EXPERIMENTAL SYSTEM

Wind tunnel testing is a prime approach to obtain and analyze aircraft aerodynamic characteristics. Results obtained from the simulation in the experimental environment can be effectively used for analyzing, calculating and improving the performances of aircraft flight. In this study, a shading enclosed experimental environment with a stroboscopic light, a photogrammetric instrument, an air blower and an air volume sensor was established, as shown in Fig. 2. This 3 dimensional detection method is mainly based upon the principle of binocular vision measurement.

A. Measurement method

Unlike traditional high speed visual measurement methods, stroboscopic imaging technique is used to record continuous image data of aircraft aerodynamic shape during its movement in one picture. The measurement speed in the experiment partly depends on the frequency of the stroboscopic light. If the frequency of the light is increasing, the images of the aircraft model overlap in the picture. If the frequency of the light is low, the images depart from each other.

As shown in Fig. 3, for simplicity, $O-XYZ$ is the world coordinate system and $o-xy$ is the image coordinate system. The transformation matrix between these two coordinate systems is a 3×4 calibration matrix C which is composed of a rotation matrix R and a translation matrix T. This calibration

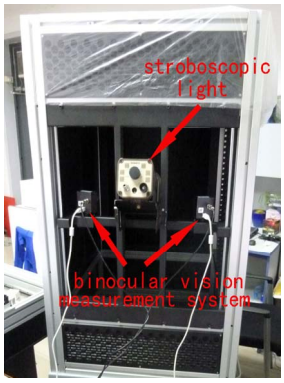

Figure 2. Experimental framework

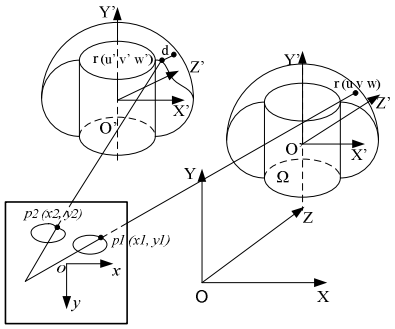

Figure 3. Coordinate System

matrix can be calculated by the Zhang's calibration method [8]. $r(u,v,w)$ refers to any point in the model coordinate system $O'-X'Y'Z'$, in which the origin is on the centroid position of the aircraft model Ω. When the model experiences the external force, its aerodynamic shape produces an elastic deformation on surface. So the location of the original point on the model coordinate changes to $r(u',v',w') = r(u,v,w) + d(u,v,w)$, where $d(u,v,w)$ is the deformation value relative to the original position of that point, as shown in Fig. 3.

B. Results

Since the stroboscopic imaging technique is used as the measurement method in the study, there will be some changes in illumination and image rotation as well as the change of scale space in the picture. Scale invariant feature transform (SIFT) is used in this study because of its flexibility. Based upon the texture information prepared on the model, SIFT features are extracted from each image respectively and their three-dimensional coordinates are also computed by the principle of binocular visual measurement. The stroboscopic image and SIFT features' spatial coordinates are presented in Fig. 4 and Fig. 5.

Figure 4. Stroboscopic image from the left camera

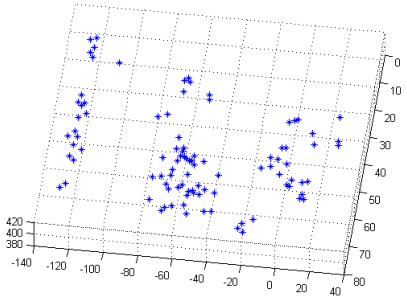

Figure 5. Three-dimensional coordinates of corresponding feature points

IV. FLIGHT STABILITY INVESTIGATION

A. Static analysis

For a deformable model, the position d, velocity $\dot{d}$, and acceleration $\ddot{d}$ are used to describe its motion property. According to the Lagrange equation of motion [9]:

$$\mu\ddot{d} + \gamma\dot{d} + \delta_d\varepsilon = f \tag{10}$$

μ represents the mass density, γ is the damping density, $\mu\ddot{d}$ is the inertial force, $\gamma\dot{d}$ is the damping force, $\delta_d\varepsilon$ is the elastic force produced due to the deformation of the model, and f is the external force acting on the model. When static situation is considered which means ignoring relative motion $\dot{d}$ and $\ddot{d}$, equation (10) can be rewritten as (11):

$$\delta_d\varepsilon = f \tag{11}$$

Here $\delta_d\varepsilon$ is a variational derivative of a deformation energy $\varepsilon(d)$, which represents the potential energy related with an elastic deformation of the model [9].

In the equation (10), if place an aircraft model under a given external force, the larger the aerodynamic shape deformation, the more elastic energy is produced on aircraft surface, the less relative motion component will be, and the better flight stability of aircraft model. It appears that increasing deformation value produced in the aircraft's aerodynamic shape helps to improve flight stability and performances of micro air vehicle during hovering in the air.

B. Effects of design parameters on the flight stabiity

Using 16 points coordinates measured from the experimental results, the parametric surface of aircraft aerodynamic shape is calculated as form (7). In the case of deformation condition, if the shape is smooth, its parametric surface can be represented by a bi-cubic patch such as (12).

$$\begin{cases} x'(u,v) = a'_{33x}u^3v^3 + a'_{32x}u^3v^2 + \cdots + a'_{00x} \\ y'(u,v) = a'_{33y}u^3v^3 + a'_{32y}u^3v^2 + \cdots + a'_{00y} \\ z'(u,v) = a'_{33z}u^3v^3 + a'_{32z}u^3v^2 + \cdots + a'_{00z} \end{cases} \tag{12}$$

$$u \in (0,1), v \in (0,1)$$

However, if using the geometry form to represent the deformation condition, the deformation component based on the original aircraft model equation (5) is unknown. If considering $\arccos\left(\frac{r}{R}\right) \le |w| \le \frac{\pi}{2}$ as the design structure, the surface (13), which contains deformation components, cannot be determined.

$$\begin{cases} x'(u,v) = \left(r - \sqrt{R^2 - \frac{H^2}{4}} + Rcosv\right)cosu + \Delta d_x(u,v) \\ y'(u,v) = \left(r - \sqrt{R^2 - \frac{H^2}{4}} + Rcosv\right)sinu + \Delta d_y(u,v) \\ z'(u,v) = Rsinv + \Delta d_z(u,v) \end{cases} \tag{13}$$

$$u \in (0,2\pi), v \in \left(-arcsin\frac{H}{2R}, arcsin\frac{H}{2R}\right)$$

Within the experiment, if the external disturbance acts on the aircraft model in X direction, the force produced in the aerodynamic shape is perpendicular to the aircraft surface. Therefore, the maximum deformation on the shape happens in X direction. So deformation component $\Delta d_y(u,v)$ in Y direction and $\Delta d_z(u,v)$ in Z direction can be ignored. Next the relationships between deformation components $\Delta d_x(u,v)$ and design parameters will be investigated and the interaction effect of parameters on the deformation variable will be analyzed.

Firstly, variable values u and v are normalized as (14):

$$\begin{cases} u' = 0.5\pi(2u-1) \in (-0.5\pi, 0.5\pi) \\ v' = \arcsin\frac{\mathrm{H}}{2\mathrm{R}}(2v-1) \in \left(-arcsin\frac{H}{2R}, arcsin\frac{H}{2R}\right) \end{cases} \tag{14}$$

$$u \in (0,1), v \in (0,1)$$

When $\arccos\left(\frac{r}{R}\right) \le |w| \le \frac{\pi}{2}$ is considered, $x(u,v)$ is given by (15):

$$x(u,v) = \left\{r - \sqrt{R^2 - \frac{H^2}{4}} + Rcos[arcsin\frac{H}{2R}(2v-1)]\right\}cos[0.5\pi(2u-1)]$$
$$u \in (0,1), v \in (0,1) \tag{15}$$

The first three terms of the Taylor series of cosine function can be used to approximate (15), which can be expanded as:

$$x(u,v) \approx \left\{r - \sqrt{R^2 - \frac{H^2}{4}} + R\left[1 - \frac{[arcsin\frac{H}{2R}(2v-1)]^2}{2!} + \frac{[arcsin\frac{H}{2R}(2v-1)]^4}{4!}\right]\right\}$$
$$\times\left\{1 - \frac{[0.5\pi(2u-1)]^2}{2!} + \frac{[0.5\pi(2u-1)]^4}{4!}\right\} \tag{16}$$

Comparing (16) with $x(u,v)$ in (7), each a_x can be calculated. In practical situations, on the half patch of the shape, the longer the distance from the acting point to the transversal surface, the smaller the deformation is. It means that in (7), when u=0 or 1, and v= 0 or 1, $x(u,v) = x'(u,v)$. Relationship among coefficients is:

$$\begin{cases} a_{03x} = a'_{03x};\ a_{02x} = a'_{02x};\ a_{01x} = a'_{01x};\ a_{00x} = a'_{00x}; \\ a_{30x} = a'_{30x};\ a_{20x} = a'_{20x};\ a_{10x} = a'_{10x}; \\ \begin{cases} a_{33x} + a_{23x} + a_{13x} = a'_{33x} + a'_{23x} + a'_{13x}; \\ a_{32x} + a_{22x} + a_{12x} = a'_{32x} + a'_{22x} + a'_{12x}; \\ a_{31x} + a_{21x} + a_{11x} = a'_{31x} + a'_{21x} + a'_{11x}; \end{cases} \\ \begin{cases} a_{33x} + a_{32x} + a_{31x} = a'_{33x} + a'_{32x} + a'_{31x}; \\ a_{23x} + a_{22x} + a_{21x} = a'_{23x} + a'_{22x} + a'_{21x}; \\ a_{13x} + a_{12x} + a_{11x} = a'_{13x} + a'_{12x} + a'_{11x}; \end{cases} \end{cases} \tag{17}$$

Deformation component $\Delta d_x\ (u, v)$ is computed by (18):

$$\Delta d_x\ (u, v) = x(u, v) - x'(u, v) \tag{18}$$

Moreover, the extreme value of $\Delta d_x\ (u, v)$ is at u=0.5, v=0.5 and the first order partial derivative $\frac{\partial \Delta d_x}{\partial u}\ (0.5,0.5)$ and $\frac{\partial \Delta d_x}{\partial v}(0.5,0.5)$ are zero. The equation of coefficients is:

$$(a_{22x} - a'_{22x}) + (a_{21x} - a'_{21x}) + 3(a_{12x} - a'_{12x}) + 3(a_{11x} - a'_{11x}) = 0 \tag{19}$$

Using coefficients equation (19), $\Delta d_{x_{max}}\ (0.5, 0.5)$ is calculated by (20):

$$\Delta d_{x_{max}}(0.5,0.5) = \frac{1}{32}(3a_{11x} - 3a'_{11x} + a_{21x} - a'_{21x}) \tag{20}$$

If the aerodynamic shape has maximum deformation, the deformation component $m = a_{21x} + 3a_{11x}$ has the maximum value as well. Substitute the above coefficients computed in this component and *m* can therefore be calculated as:

$$m = 2R\pi^2(arcsin\frac{H}{2R})^2 - \frac{1}{3}R\pi^2(arcsin\frac{H}{2R})^4 \tag{21}$$

The interaction effect of the design parameters *H* and *R* in the deformation component can be estimated from Fig. 6. It appears that a small external radius *R* and a large height *H* will increase the value of deformation component *m,* which will also result in better flight stability due to large elastic deformation in the aircraft aerodynamic shape.

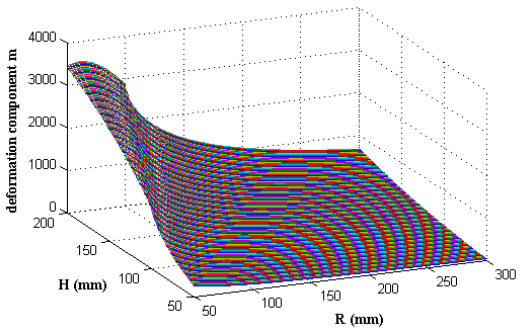

Figure 6. Interaction effect of height *H* and external radius *R*

V. CONCLUSIONS

The investigation of flight stability is a constituent part in the aircraft structure design stage. In particular, the design parameters also determine the flight characteristics and properties of ducted-fan hovering MAVs. In order to improve the stability, different designed parametric vertical ducted-fan hovering aircrafts with elastic aerodynamic shape have been presented and discussed. Within such aircraft model, stroboscopic imaging technique was proposed in the experimental measurement system to obtain the three-dimensional information of the shape. One of the key advantages of this approach is to record and track moving objects without using high-speed imaging equipment. The features extracted from the shape were used to define the parametric surface of the shape. Through comparing parameters between algebraic and geometric forms of the surface definition, the relationship between designed structural parameters and flight stability has been analyzed and calculated mathematically. It was found that increasing the height of vertical ducted-fan and decreasing the external radius of the shell seem to produce a larger deformation in the aerodynamic shape. It means that the flight stability will be improved if the interaction effects of designed parameters are considered.

ACKNOWLEDGMENT

This work was supported by Specialized Research Fund for the Doctoral Program of Higher Education (SRFDP), China.

REFERENCES

[1] B. J. Tsai and Y. C. Fu, "Design and aerodynamic analysis of a flapping-wing micro aerial vehicle," Aerospace Science and Technology, vol. 13, pp. 383-392, October-November 2009.

[2] T. Kanade, O. Amidi, and Q. Ke, "Real-time and 3D vision for autonomous small and micro air vehicles," 43rd IEEE Conference on Decision and Control Bahamas, vol. 2, pp. 1655-1662, December 2004.

[3] R. J. Bachmann, F. J. Boria, R. Vaidyanathan, P. G. Ifju, and R. D. Quinn, "A biologically inspired micro-vehicle capable of aerial and terrestrial locomotion," Mechanism and Machine Theory, vol. 44, pp. 513-526, March 2009.

[4] J. M. Pflimlin, P. Soueres, and T. Hamel, "Hovering flight stabilization in wind gusts for ducted fan UAV," 43rd IEEE Conference on Decision and Control Bahamas, vol. 4, pp. 3491-3496, December 2004.

[5] Z. Zhang and P. Q. Liu, "The experiment reseatch on the MAV aerodynamic character effected by planforms," Aircraft Design, vol. 29, pp. 1-5, 2009.

[6] R. Albertani, B. Stanford, J. P. Hubner, and P. G. Ifju, "Aerodynamic coefficients and deformation measurements on flexible micro air vehicle wings," Experimental Mechanics, vol. 47, pp.625-635, 2007.

[7] E. N. Johnson and M. A. Turbe, "Modeling, control, and fight testing of a small ducted fan aircraft," AIAA Guidance, Navigation, and Control Conference and Exhibit California, pp. 1-23, August 2005.

[8] Z. Y. Zhang, "A flexible new technique for camera calibration," IEEE Transaction on Pattern Analysis and Machine Intelligence, vol. 22, pp. 1330-1334, 2000.

[9] D. Terzopoulos and A. Witkin, "Physically based models with rigid and deformable components," Computer Graphics and Applications, vol. 8, pp. 41-51, November 1988.